

University of Kentucky

UKnowledge

---

Mechanical Engineering Faculty Publications

Mechanical Engineering

---

2019

## Computationally Efficient, Multi-Domain Hybrid Modeling of Surface Integrity in Machining and Related Thermomechanical Finishing Processes

Julius M. Schoop

*University of Kentucky*, [julius.schoop@uky.edu](mailto:julius.schoop@uky.edu)

David Adeniji

*University of Kentucky*, [dadeniji@uky.edu](mailto:dadeniji@uky.edu)

Ian S. Brown

*University of Kentucky*, [iansbrowninc@gmail.com](mailto:iansbrowninc@gmail.com)

Follow this and additional works at: [https://uknowledge.uky.edu/me\\_facpub](https://uknowledge.uky.edu/me_facpub)



Part of the [Mechanical Engineering Commons](#)

**Right click to open a feedback form in a new tab to let us know how this document benefits you.**

---

### Repository Citation

Schoop, Julius M.; Adeniji, David; and Brown, Ian S., "Computationally Efficient, Multi-Domain Hybrid Modeling of Surface Integrity in Machining and Related Thermomechanical Finishing Processes" (2019). *Mechanical Engineering Faculty Publications*. 70.

[https://uknowledge.uky.edu/me\\_facpub/70](https://uknowledge.uky.edu/me_facpub/70)

This Conference Proceeding is brought to you for free and open access by the Mechanical Engineering at UKnowledge. It has been accepted for inclusion in Mechanical Engineering Faculty Publications by an authorized administrator of UKnowledge. For more information, please contact [UKnowledge@lsv.uky.edu](mailto:UKnowledge@lsv.uky.edu).

---

# Computationally Efficient, Multi-Domain Hybrid Modeling of Surface Integrity in Machining and Related Thermomechanical Finishing Processes

Digital Object Identifier (DOI)

<https://doi.org/10.1016/j.procir.2019.03.225>

## Notes/Citation Information

Published in *Procedia CIRP*, v. 82.

© 2019 The Author(s)

Under a Creative Commons [license](#)

17th CIRP Conference on Modelling of Machining Operations

# Computationally efficient, multi-domain hybrid modeling of surface integrity in machining and related thermomechanical finishing processes

Julius Schoop<sup>a\*</sup>, David Adeniji<sup>a</sup>, Ian Brown<sup>a</sup>

<sup>a</sup>Department of Mechanical Engineering and Institute for Sustainable Manufacturing, University of Kentucky, Lexington, USA

\* Corresponding author. Tel: +1-859-323-8308; fax: +1-859-257-1071. E-mail address: [julius.schoop@uky.edu](mailto:julius.schoop@uky.edu)

## Abstract

In order to enable more widespread implementation of sophisticated process modeling, a novel, rapidly deployable multi-physics hybrid model of surface integrity in finishing operations is proposed. Rather than modeling detailed chip formation mechanics, as is common in numerical models, the proposed models integrates existing analytical and semi-empirical models of the plastic, elastic, thermal and thermodynamic domains. Using this approach, highly complex surface integrity phenomena such as residual stresses, grain size, phase composition, microhardness profile, etc. can be accurately predicted in a manner of seconds. It is envisioned that this highly efficient modeling scheme will drive new innovations in surface engineering.

© 2019 The Authors. Published by Elsevier B.V.

Peer-review under responsibility of the scientific committee of The 17th CIRP Conference on Modelling of Machining Operations

*Keywords:* Surface Integrity; Hybrid Modeling; Finishing; Surface Engineering; Digital Design

## 1. Introduction

Modelling of machining and finishing operations such as grinding, burnishing and polishing is crucial to the development of more efficient and sustainable products and processes. Machining is a highly complex process involving phenomena traditionally studied in the fields of mechanics, thermodynamics, tribology, industrial engineering, and more recently, materials and surface engineering. Much effort has been devoted to modelling of cutting forces and tool-wear and tool-life [1]; indeed, the earliest models and studies by Frederick Taylor were concerned with this very topic. Considering the significant cost of cutting tools and the necessity for increased productivity and process security, tool-life is clearly an important phenomenon to model and predict.

More recently, with the advent of near-net shape manufacturing techniques such as precision casting and additive manufacturing, a trend towards finishing processes has been emerging. The unparalleled ability of machining processes to produce excellent dimensional tolerances, surface finishes at industrial scales and reasonable cost has established

these processes as the most versatile technique for precision finishing.

However, traditional models of cutting forces and tool-wear do not address the key metric of finishing processes, i.e. product quality, which is often assessed in terms of surface integrity. It is now well-established that the thermo-mechanical process of machining and related processes such as polishing, burnishing and grinding, all have an important impact on the surface and sub-surface properties of machined components, such as grain size, phase composition, hardness and residual stresses [2]. However, as will be shown in the ensuing discussion, current modelling approaches of surface integrity, most notably finite element (FEM) simulations, are limited in their predictive power and accuracy [3]. Even more importantly, numerical simulations generally require significant computational time. Therefore, a key objective of the proposed study is to develop a truly predictive and computationally-efficient (i.e., real-time) model of surface integrity induced by finishing processes.

In order to fully leverage the ability of finish machining processes to not only produce geometrical features but also to engineer to surface and sub-surface properties of machined

components, there is a need for a new paradigm of reverse modeling. Rather than having process parameters as inputs and the resultant surface integrity parameters as outputs (the forward modeling approach), reverse modeling relies on desirable design characteristics, e.g. a residual stress profile, as inputs and process parameters become outputs. To achieve reverse modeling, the development of high-speed, high-accuracy predictive models is a necessary first condition. Considering on the shortcomings of current models, most importantly the uncertainty surrounding friction and flow stress as documented in a recent CIRP keynote paper by Melkote et al. [4], a mechanistic hybrid modelling approach is proposed to finally leverage the machining process as a material characterization test, as was envisioned by pioneers such as P.B. Oxley more than half a century ago [5, 6]. Using advanced, ultra-high speed microscopy and digital image correlation algorithms, friction and flow stress data can be obtained in-situ and at realistic speeds of several meters per second. Notable prior research was performed at only millimeters per seconds, in order to obtain sufficiently detailed flow fields [7].

## 2. Experimental Setup

Experimental data was collected using a proprietary ultra-high speed microscopy testbed developed at the University of Kentucky. By employing the very latest generation of CMOS high resolution (2 Mpx), ultra-high throughput (16 Gpx/sec) sensor technology (iX cameras i-speed 726) and a custom-built ultra-high intensity LED liquid light guide optic light source (>250 million lux), the system is capable of obtaining nanosecond exposure microscopic images at realistic cutting speeds ( $v_c = 50\text{--}250$  m/min) and frame rates up to 1,000,000 per second. The ultra-high speed camera is connected to a high resolution video microscope manufactured by Mitutoyo (VMU-V) and can be reliably used up to 50x magnification. The maximum spatial resolution of the system, considering optical (Rayleigh/diffraction) and sensor (Nyquist/sampling) limitations, is approximately 550 nm, i.e. the wavelength of visible light. Therefore, very small strains and very high strain rates, up to  $\dot{\epsilon} = 10^8$  can be resolved. At the same time, very high strains, up to  $\epsilon = 10,000\%$  can likewise be resolved using custom digital image correlation software (DIC) in Matlab.

The ultra-high speed microscopy system is used in conjunction with a high speed linear stage capable of more than 5 Gs of acceleration and 4 m/s peak speeds with 50 nm absolute encoder feedback to enable in-situ generation of highly detailed image sequences. Analysis of these sequences using DIC reveals complex strain and strain rate fields, which in turn can be correlated with synchronized force, vibration, thermal, etc. data collected using a variety of sensors such as high resolution strain gages, accelerometers and infrared pyrometers and thermocouples. Thus, the custom-developed testbed enables detailed characterization of dynamic material behaviour during the machining process across a variety of physical properties and domains. The testbed was specifically developed with the intent to leverage the machining/finishing process itself as a more accurate material property characterization technique. The manner in which this vision is being currently realized will be laid out in the following discussion.

## 3. Proposed Mechanistic Hybrid Model

### 3.1. Necessity of a multi-domain approach for modelling of thermomechanical finishing processes

When developing a computationally-efficient model, it is first necessary to reduce the process being modelled down to its most fundamental essence. Considering the fact that most metal finishing processes share the same fundamental physics, it is possible to generalize and categorize these processes based on their shared archetypal essence. For example, the transition from chip-less processes, such as polishing and burnishing, to chip generation processes such as grinding and machining, occurs on a spectrum. Concepts such as the minimum chip thickness or critical indentation pressure can be used to draw the transitional boundaries between sliding, ploughing and removal regimes [8]. However, the fundamental process geometry and thermomechanical loads are shared across the various regimes, although to greatly varying degrees and with markedly different results. Fig. 1 qualitatively summarizes the domains that characterize machining and finishing processes.

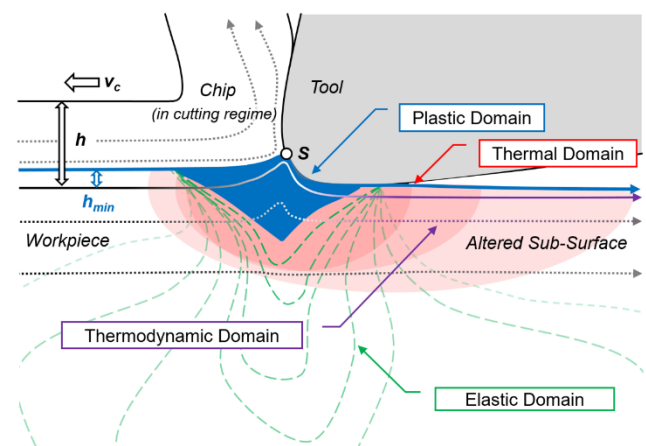


Fig. 1: Schematic overview of the four major domains that archetypically characterize thermomechanical finishing processes.

### 3.2. Multi-physics semi-empirical constitutive model

As can be seen in Fig. 1, there are four major domains associated with thermomechanical finishing processes. Realistic constitutive modelling of material behaviour needs to therefore include aspects addressing each of these domains. In other words, simple elastic/plastic constitutive modelling, as provided by common models as the one initially developed by Johnson and Cook, is inadequate for describing the dynamic changes that occur during thermomechanical processing [9]. Even more importantly, input data for Johnson Cook model parameters are often derived from loading geometries that are fundamentally different from real finishing processes, e.g. high strain rate tensile, pressure plate, or Split Hopkinson bar tests. The boundary conditions and states of hydrostatic stress, thermal gradients, strain rates, etc. encountered during finishing processes are strongly interrelated and as such cannot be modelled effectively using traditional mechanical characterization tests and constitutive models.

Rather than using single-domain constitutive models, a

physics-based hybrid modelling approach, with relevant inputs provided by the process itself (i.e., in-situ) is being proposed as an alternative to current modelling schemes. Using such high quality experimental inputs, as well as a de-coupled (superposition) scheme, high-speed multi-domain modelling can be achieved. In this hybrid model, experimental data is used to quasi-couple and scale the various domains' sub-models.

The following discussion will focus on laying out specifics of the various sub-models for each of the four major domains in thermomechanical finishing processes. It should be noted that since the process of surface generation occurs below the separation point  $S$  (see Fig. 1), the influence of the chip on the tool as well as on the final/finished workpiece surface will be neglected. This assumption is generally only reasonable at small values uncut chip thickness, which are however one of the key characteristics of finishing processes. Since the focus of this work lies in computationally-efficient modelling of surface integrity in finishing processes, the proposed model was intentionally constructed to achieve this specific objective.

### 3.3. Thermal domain sub-model

Since the physical, thermodynamic and mechanical properties of materials are strongly dependent upon temperature, the first step in generating the proposed multi-physics model is calculation of a preliminary thermal field. This field is preliminary since subsequent calculation of mechanical (elastic and plastic effects, e.g. hydrostatic stress and strain accumulation/hardening) as well as thermodynamic effects (grain refinement, phase transformations, etc.) can lead to altered physical properties such as thermal conductivity and heat capacity. These changes alter the thermal field, which alters the mechanical and thermodynamic response, and so on. Without explicit coupling of the various regimes, which the proposed model intentionally avoids in order to maintain computational efficiency, there is a need for limited iterations to obtain a quasi-coupled model output. To begin this process, a preliminary thermal field needs to be provided.

Considering the various sources of heat generation during finishing processes, the influence of frictional heating in the tertiary shear zone (i.e., in the plastic domain underneath the tool's flank) was considered to be of chief importance with respect to surface integrity. While the heat generated due to plastic deformation in the primary shear zone and frictional heating on the rake face in the secondary shear zone accounts for the majority of the heat generated, this heat also tends to be carried away by the chip (in chip generating processes) or be absorbed by the tool to some degree. In chipless processes, e.g., burnishing and polishing, the tertiary shear zone is to some extent equivalent to the microscopic effect of frictional heating, i.e., localized plastic deformation.

In tribology, the temperature profile generated during sliding contact is considered to be chiefly affected by the dimensionless Péclet number, which signifies the ration of the rate of advective transport to that of diffusive transport [10]. As such, it is strongly affected by material properties. In finishing processes, we can define:

$$Pe = \frac{v_c b \rho c_p}{2k} \quad (1)$$

Where  $b$  is the half-width of contact between the workpiece and tool,  $\rho$  is the density of the workpiece material,  $c_p$  is the specific heat capacity of the workpiece material and  $k$  the thermal conductivity.

At high values of  $Pe$ , i.e.,  $Pe > 5$ , as is common in materials with poor thermal conductivity (e.g., titanium alloys) and high cutting speeds, the thermal field will have a high peak (flash) temperature and low penetration into the workpiece. This case is thus highly dynamic and deviates from thermal equilibrium, which generally occurs at values of  $Pe < 0.2$ , i.e., at very low cutting speeds for materials with high thermal conductivity and low heat capacity. Under these latter conditions, the thermal field will be approximately symmetrical about the frictional contact area. Higher  $Pe$  values distort the thermal field towards the trailing edge of the tool (i.e., the flank) and cause elongation of the highest value isotherms on the recently processed surface, as illustrated in Fig. 2.

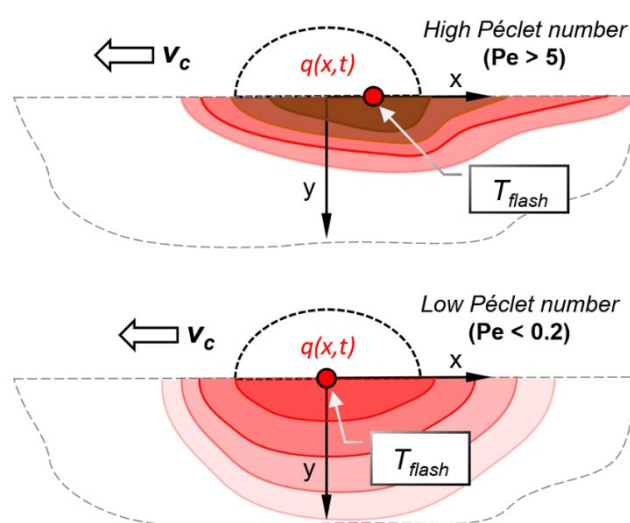


Fig. 2: Schematic overview of the thermodynamic domain, illustrating the qualitative effect of the Péclet number on the thermal field.

When calculating  $Pe$ , the dynamic physical values of  $c_p$  and  $k$ , both of which are strongly influenced by temperature and hydrostatic stress, need to be considered. Given reasonably accurate determination of  $Pe$ , the normalized thermal field on the surface can be calculated using a quasi-static solution the transient heat equation through the modified Bessel Equations of the second kind,  $K_0$  and  $K_1$ .

A convenient solution to this complex problem has been presented by Liu et al. [11], who proposed the use of normalized influence coefficients to provide a solution for quasi-steady state surface heating of the half-plane. It should be noted that the time to reach the steady state conditions again depends strongly on  $Pe$ , but varies roughly between 1 to 0.1 s. Thus, the proposed thermal field will deviate from the real (transient) distribution highly dynamic processes such as high speed milling or interrupted turning. In these cases, a significantly more complex approach is required for arcuate prediction of the thermal field. Since many finishing processes can however be considered to feature approximately steady-state conditions, this approach was used within the context of the proposed model. Following Liu et al.'s the normalized surface temperature profile may be expressed via Equation (2).

$$T_{ss}(x, 0) = \frac{1}{\max T_{ss}} \begin{cases} \left\{ \begin{array}{l} (x+b)e^{P_+}[K_0(-P_+) - K_1(-P_+)] \\ +(b-x)e^{P_+}[K_0(-P_-) - K_1(-P_-)] \end{array} \right\} & x \leq -b \\ \left\{ \begin{array}{l} (x+b)e^{P_+}[K_0(P_+) + K_1(P_+)] \\ +(b-x)e^{P_-}[K_0(-P_-) - K_1(-P_-)] \end{array} \right\} & -b \leq x \leq b \\ \left\{ \begin{array}{l} (x+b)e^{P_+}[K_0(P_+) + K_1(P_+)] \\ +(b-x)e^{P_-}[K_0(P_-) + K_1(P_-)] \end{array} \right\} & b \leq x \end{cases} \quad (2)$$

$$\text{where } P_{\pm} = \frac{Pe(x \pm b)}{2} \quad (3)$$

To scale the normalized thermal field, the flash temperature  $T_{flash}$  can be calculated for the two Péclet regimes according to the semi-empirical relations in Equation (4).

$$T_{flash} = \begin{cases} (8.38 * 10^{-4}Pe^3 - 0.031Pe^2 + 0.380Pe) * \left(\frac{2F_N}{\rho c_p w b}\right), & Pe \leq 5 \\ 0.399 * \left(\frac{2F_N v_c}{kw}\right) \sqrt{\frac{k}{\rho c_p v_c b}}, & Pe > 5 \end{cases} \quad (4)$$

where  $F_N$  is the normal force (feed force in orthogonal machining) and  $w$  the width of contact, perpendicular to the cutting and feed directions.

Given the shape of the surface temperature profile from Eqs. 2-4, the sub-surface temperature profile for each surface point at sub-surface depths  $y$  and surface points  $x$  (relative to the center point of tool/workpiece contact at  $x = 0$ ) may be reasonably approximated using the solution to the simple one-dimensional quasi-stationary line heat source problem as:

$$T(x, y) = T_{ss}(x, 0) * \left\{ 1 - \operatorname{erf}\left(\frac{y}{\sqrt{\frac{2 \rho k}{v_c c_p b}}}\right) \right\} \quad (5)$$

where  $\operatorname{erf}$  represents the error function, which results from integrating the normal distribution. Equation (5) provides a closed-form expression for the entire thermal field due to frictional heating in plane-strain (i.e., 2D) conditions. It represents a starting point for the calculation of other relevant values calculated through other sub-models, which will be discussed in the following sections.

### 3.4. Plastic domain sub-model and severe plastic deformation

As evident from the schematic shown in Fig. (1), the plastic domain is of central importance to the nature of thermomechanical finishing processes. Within this domain, the workpiece material may be subjected to strains up to 1000%, with similarly extreme temperature and strain rate gradients. All of these effects can significantly alter the workpiece microstructure through severe plastic deformation and associated phase transformations and grain refinement. While these latter effects are fundamentally thermodynamic in nature, i.e. the subject of yet another domain, the material behavior within the plastic domain needs to first be understood in order to model and predict resultant thermodynamic changes.

A well-developed analytical technique for modeling of

finite (i.e., large) strains is slip line modeling. Slip lines represent the physical planes along which plastic deformation occurs via slip, as is the case in metals. In processes such as drawing, forging, etc. the use of slip line models has long been demonstrated to be highly predictive, since the basic model assumption (perfect plastic material behavior, free/adhesive interface boundary conditions, etc.) are fundamentally reasonable. In machining, several researchers have developed and modified slip line modeling in order to better represent the highly complex boundary conditions that occur during chip-generating processes [12, 13]. Within the context of the proposed model, a simpler approach was adopted by limiting the scope to finishing processes.

The earliest attempt to characterize the slip line geometry and characteristics in finishing processes was undertaken by Challen and Oxley [8]. The single and double-chord models proposed by Challen and Oxley fail to accurately represent the more complex geometries of real cutting tools with variable edge preparations, chip breakers, coatings, etc. However, the model happens to represent the physical realities of finishing processes, i.e. highly negative effective rake angle due to the small ratio of uncut chip thickness to (equivalent) cutting edge radius, quite well. As such, the assumption of a negative rake angle wedge may be taken as a reasonable assumption for the contact geometry between the tool and workpiece material under sliding, ploughing and burnishing/polishing conditions. Since these regimes are characteristic of finishing processes, predictions made by Challen and Oxley's single chord model (see Fig. 3 below) may be used to approximate the shape and properties of the plastic domain in finishing.

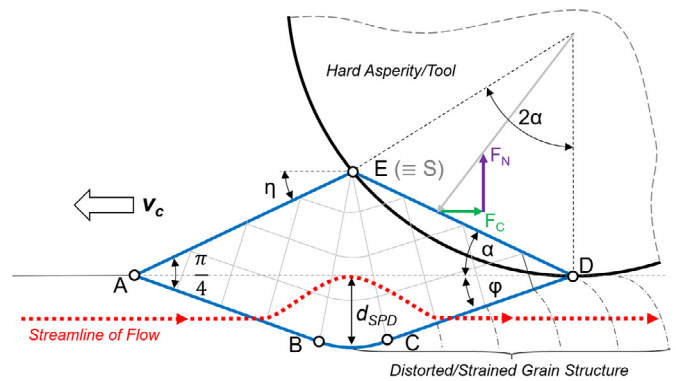


Fig. 3: Oxley and Challen's single chord slip line model.

From the simple single chord slip line model, several calculations may be performed. The depth of the plastic deformation ( $d_{SPD}$ ) can be approximated via Equation (6) as:

$$d_{SPD} \cong x_1 * \frac{\tan\left(\frac{\pi}{4} - \eta\right)}{\tan\left(\frac{\pi}{4} - \eta\right) + \tan(x_1)} * \tan\left(\frac{\arccos(\mu)}{2} - \alpha\right) \quad (6)$$

$$\text{where: } x_1 = S \left( \sqrt{\frac{1 - \sin^2(\eta)}{\sin^2(\eta)}} + \sqrt{\frac{1 - \sin^2(\alpha)}{\sin^2(\alpha)}} \right) \quad (7)$$

$$\eta = \arcsin\left(\frac{\sin(\alpha)}{\sqrt{1 - \mu}}\right), \quad \mu = \frac{F_C}{F_N} \quad (8)$$

Moreover, the maximum plastic deformation, grain tilt

angle (i.e. path difference between plastic surface and elastic sub-surface layers) and friction coefficient may all be implicitly calculated. Given the limited space within the present manuscript, this capability was illustrated schematically in Fig 3. It should be noted that exact calculation of the grain tilt geometry requires knowledge of the flow stress and friction during every point within the plastic (i.e., slip line) field. Practically, this requires in-situ experimental data along with a sophisticated constitutive model, as discussed previously.

### 3.5. Elastic domain sub-model and residual stresses

Within the elastic/plastic mechanical domain(s), the material is first loaded elastic until it reaches its yield point and then flows for some distance at some value of flow stress, during which the mechanical properties may change due to strain hardening, thermal softening and/or thermodynamically induced phase transformations. As the tool passes over a region of the workpiece material's sub-surface, a given point within this sub-surface will be loaded and then unloaded. Under certain circumstances, specifically in cases where a residual plastic strain is accumulated during this complex loading/unloading processes, the material will retain a certain residual stress [14]. It should be noted that this residual stress cannot exceed the (current) yield strength of the material. However, due to strain hardening, thermal softening, etc., this yield strength may differ significantly from the virgin state, i.e., prior to thermomechanical processing.

In order to accurately predict residual stresses, the precise stress/strain history of a given particle within the workpiece material needs to be known and considered. Within the elastic domain, material does not flow, which means that following an elastically loaded/unloaded particle is as simple as calculating the state of stress and strain along a straight (horizontal) line. Whatever strain is accumulated after the tool has passed will remain and cause a corresponding residual stress. For material within the severe plastic deformation depth ( $d_{SPD}$ ), the situation is significantly more complicated; material flows both vertically and horizontally and at a speed different from the cutting speed, due to viscous shear. Consequently, calculating residual stresses for particles passing through the plastic domain requires more complex calculations.

The state of stress beneath a sliding cylinder over an elastic half space (i.e., under plain strain conditions) can be calculated quite readily using the Hertz theory. Clearly, the assumptions made by this theory are not representative of the overall conditions encountered in either metal cutting or even burnishing, primarily due to the complex material behavior that results from local plasticity, varying/evolving constitutive properties and frictional interactions and heating. Nevertheless, by limiting the scope of the Hertz theory to the elastic domain, it is possible to obtain rapidly solved (i.e., closed-form) expressions for the state of stress within the half space.

Even more importantly, by employing a sophisticated constitutive model and through iterative adjustments of the state of stress due to strain hardening, thermal softening, strain rate hardening, etc., it is possible to further improve the outputs for the elastic unloading behavior of the workpiece sub-surface.

The state of elastic (i.e. infinitesimal strain) stress beneath the sub-surface can be expressed in normalized form, i.e. scaled by the half width of contact  $a$  via Equations (9-11), following McEwen's [15] convention in terms of  $m$  and  $n$  (Eqs. 12-13).

$$\sigma_x = -\frac{p_0}{a} \left\{ m \left( \left( 1 + \frac{z^2+n^2}{m^2+n^2} \right) - 2y \right) + \left( \mu * \text{sgn}(x) \left( n \left( 2 - \frac{y^2-m^2}{m^2+n^2} \right) - 2x \right) \right) \right\} \quad (9)$$

$$\sigma_y = -\frac{p_0}{a} \left\{ m \left( 1 - \frac{z^2+n^2}{m^2+n^2} \right) + \mu \left( n \left( \frac{m^2-y^2}{m^2+n^2} \right) \right) \right\} \quad (10)$$

$$\tau_{xy} = -\frac{p_0}{a} \left\{ n * \text{sgn}(x) \left( \frac{m^2-y^2}{m^2+n^2} \right) + \left( \mu m \left( \left( 1 + \frac{z^2+n^2}{m^2+n^2} \right) - 2y \right) \right) \right\} \quad (11)$$

With  $m$  and  $n$  defined as:

$$\frac{m^2}{a^2} = \frac{1}{2} \left[ \left( \sqrt{\left( 1 + \left( \frac{z}{a} \right)^2 \right)^2 - 2 \left( 1 + \left( \frac{z}{a} \right)^2 \right) * \left( \frac{x}{a} \right)^2 + \left( \frac{x}{a} \right)^4 + 4 \left( \frac{z}{a} \right)^2 \left( \frac{x}{a} \right)^2} \right) + 1 + \left( \frac{z}{a} \right)^2 - \left( \frac{x}{a} \right)^2} \right] \quad (12)$$

$$\frac{n^2}{a^2} = \frac{1}{2} \left[ \left( \sqrt{\left( 1 + \left( \frac{z}{a} \right)^2 \right)^2 - 2 \left( 1 + \left( \frac{z}{a} \right)^2 \right) * \left( \frac{x}{a} \right)^2 + \left( \frac{x}{a} \right)^4 + 4 \left( \frac{z}{a} \right)^2 \left( \frac{x}{a} \right)^2} \right) - 1 - \left( \frac{z}{a} \right)^2 + \left( \frac{x}{a} \right)^2} \right] \quad (13)$$

### 3.6. Thermodynamic domain sub-model

The thermodynamic domain is arguably the most complex phenomenon to properly model, yet also happens to be governed by the most concise principle. A variety of complex and heavily interdependent effects give rise to phenomena such as dynamic recrystallization and phase changes. However, with the approximation of incompressibility (i.e., at constant volume) these irreversible phenomena are fundamentally governed by the Helmholtz Free Energy,  $A$ . The differential of  $A$ , for a process with no change in the number of particles, is defined in terms of the internal energy  $U$ , absolute temperature  $T$  and Entropy  $S$  as shown in Equation (14).

$$dA \equiv dU - TdS = V \sum_{ij} \sigma_{ij} d\varepsilon_{ij} - S dT \quad (14)$$

Based on the principle of minimum energy, a reduction in  $A$  corresponds to a spontaneous process, with the lowest attainable value of  $A$  being the equilibrium state of a system. In other words, any change of state leading to reduced Helmholtz Free Energy during thermomechanical processing will be thermodynamically possible, although kinetic limitations may still prevent such changes from occurring. By calculating  $A$  at each point for a particle traveling underneath a tool during a finishing process, it is possible to accurately predict phase changes and similar phenomena. It should be noted that this approach has also been successfully employed by Buchkremer and Klocke [9] to model surface integrity in AISI 4140 steel.

## 4. Results and Discussion

### 4.1. Scope and limitations of the proposed model

Since one of the primary objectives of the work presented here is to enable computationally-efficient (i.e., fast/real-time) modeling of thermomechanical finishing processes, the proposed model was constructed with a focus on process-induced surface integrity. Chip formation phenomena, as well as detailed cutting force and tool wear simulation are outside the scope of the present model. Moreover, the multi-domain approach espoused here relies on coupling of fundamentally de-coupled theories and regimes. Therefore, it is necessary to use high-quality empirical input data from in-situ ultra-high speed imaging, as described in the experimental setup section. Going forward, improved heuristics and integration of advanced machine-learning algorithms is envisioned to greatly reduce the reliance on experimental inputs, particularly once sufficient ‘teaching data’ will be available for a machine-learning algorithm.

### 4.2. Preliminary validation of the proposed model

The proposed model has already been studied and preliminarily validated in Ti-Alloy *Ti-6Al-4V*. Surface integrity data obtained in orthogonal machining (turning), along with corresponding model predictions, is summarized in Fig. 4. It should be noted that the time to calculate these outputs was approximately one second.

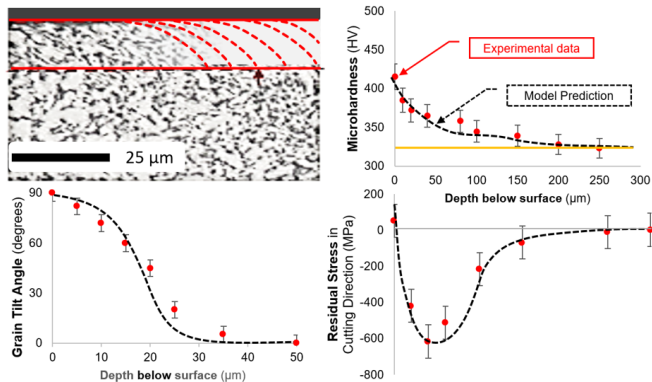


Fig. 4: Representative validation of proposed model in cryogenic machining of *Ti-6Al-4V* with  $v_c = 60$  m/min,  $f = 0.05$  mm/rev,  $r_\beta = 25$   $\mu$ m.

## 5. Summary and Conclusions

In summary, a new computationally-efficient predictive model of surface integrity from thermomechanical finishing processes was developed. Using a hybrid, empirical/analytical (mechanistic) approach, it was shown that reasonably accurate ( $\pm 10\%$ ) and highly detailed surface integrity profiles can be obtained in a manner of seconds, including notoriously difficult-to-model residual stresses. Therefore, the proposed modeling technique is envisioned to be highly relevant to industry, particularly high value-added enterprises in the automotive, aerospace and biomedical sectors. By reducing computational time in modeling of process-induced surface integrity, industry will be able to develop new generations of

products with engineered surface quality. Subsequent work will focus on expanding and validating the model in finishing of steel, aluminum, and nickel alloys.

## References

1. Van Luttervelt, C., et al., *Present situation and future trends in modelling of machining operations progress report of the CIRP Working Group 'Modelling of Machining Operations'*. CIRP Annals - Manufacturing Technology, 1998. **47**(2): p. 587-626.
2. Jawahir, I., et al., *Surface integrity in material removal processes: Recent advances*. CIRP Annals-Manufacturing Technology, 2011. **60**(2): p. 603-626.
3. Arrazola, P., et al., *Recent advances in modelling of metal machining processes*. CIRP Annals-Manufacturing Technology, 2013. **62**(2): p. 695-718.
4. Melkote, S.N., et al., *Advances in material and friction data for modelling of metal machining*. CIRP Annals - Manufacturing Technology, 2017. **66**(2): p. 731-754.
5. Palmer, W. and P. Oxley, *Mechanics of orthogonal machining*. Proceedings of the Institution of Mechanical Engineers Part C-Journal of Mechanical Engineering Science, 1959. **173**(1): p. 623-654.
6. Stevenson, M. and P. Oxley, *An experimental investigation of the influence of strain-rate and temperature on the flow stress properties of a low carbon steel using a machining test*. Proceedings of the Institution of Mechanical Engineers, 1970. **185**(1): p. 741-754.
7. Guo, Y., W.D. Compton, and S. Chandrasekar, *In situ analysis of flow dynamics and deformation fields in cutting and sliding of metals*. J Proc. R. Soc. A, 2015. **471**(2178): p. 20150194.
8. Challen, J. and P. Oxley, *Slip-line fields for explaining the mechanics of polishing and related processes*. International Journal of Mechanical Sciences, 1984. **26**(6-8): p. 403-418.
9. Buchkremer, S. and F. Klocke, *Modeling nanostructural surface modifications in metal cutting by an approach of thermodynamic irreversibility: Derivation and experimental validation*. Continuum Mechanics Thermodynamics, 2017. **29**(1): p. 271-289.
10. Kennedy, F.E., *Frictional heating and contact temperatures*. Modern tribology handbook. Vol. 1. 2001. 235-272.
11. Liu, S., et al., *Solutions for temperature rise in stationary/moving bodies caused by surface heating with surface convection*. J Journal of heat transfer, 2004. **126**(5): p. 776-785.
12. Roth, R. and P. Oxley, *Slip-line field analysis for orthogonal machining based upon experimental flow fields*. Journal of Mechanical Engineering Science, 1972. **14**(2): p. 85-97.
13. Fang, N., I. Jawahir, and P.J.I.J.o.M.S. Oxley, *A universal slip-line model with non-unique solutions for machining with curled chip formation and a restricted contact tool*. 2001. **43**(2): p. 557-580.
14. Johnson, K.L., *Contact mechanics*. 1987: Cambridge university press.
15. McEwen, E., *Stresses in elastic cylinders in contact along a generatrix*. Philosophical Magazine, 1949. **40**: p. 454-460.